CAV2009 – Paper No. 146

Control Experiments with a Semi-Axisymmetric Supercavity and a Supercavity-Piercing Fin

Martin Wosnik
Department of Mechanical Engineering
University of New Hampshire
Durham, NH 03824, U.S.A

Roger E.A. Arndt
St. Anthony Falls Laboratory
University of Minnesota
Minneapolis, MN 55405, U.S.A

ABSTRACT

Supercavitation can significantly reduce skin-friction drag on an underwater body, thus enabling a dramatic increase in attainable velocity. The control of a High-Speed Supercavitating Vehicle (HSSV) poses unique challenges, since only small regions at the nose (cavitator) and on the afterbody (fins) are in contact with water and can be used as control surfaces. The interaction between supercavity dynamics and control surface actuation is complex and nonlinear.

Experiments were conducted with a semi-axisymmetric, ventilated supercavity and a single wedge-shaped, 45 degree swept, cavity-piercing fin in the high-speed water tunnel at St. Anthony Falls Laboratory. Motion control was combined with water tunnel testing to create a "hardware-in-the-loop" system that can (a) provide critical hydrodynamic parameters for control models and (b) serve as a test bed for fin control strategies. Through a series of experiments, control surface-cavity interaction, cavity stability and hysteresis effects were studied. Fin torque (lift) was measured for different angles of attack with varying cavitation numbers. Closed-loop fin control experiments simulating simple maneuvers were carried out.

INTRODUCTION

Supercavitation[1] can significantly reduce skin-friction drag on bodies moving through water. Supercavitation applications include propellers, pumps, hydrofoils, projectiles and controllable vehicles, such as torpedoes. A cavitator at the front of a supercavitating vehicle, typically disk- or cone-shaped, is designed to create a cavity of sufficient size to envelop the entire vehicle body. If the vehicle travels fast enough for the cavitator to reduce pressure dynamically to vapor pressure, then the cavity can be sustained with water vapor alone (*natural* or vaporous supercavitation). In all other cases, including startup and maneuvers, additional ventilation, for example using

---

[1] A "super"-cavity is a large, attached cavitation bubble that extends beyond the object that generates it.

propulsion exhaust gas, is necessary (*artificial* or gaseous supercavitation). In other words, for supercavitation to occur a certain, low cavitation number must be reached and maintained. A low cavitation number based on cavity pressure can be achieved through high vehicle velocity or, alternatively, by an increase in cavity pressure through ventilation.

The control of a supercavitating vehicle poses unique challenges, since only small regions at the nose (cavitator) and on the afterbody (fins, and/or planing) are in contact with water. Unlike for a fully wetted torpedo, there is an absence of hydrodynamic lift on the body. The weight of the vehicle must be supported by lift generated by the cavitator (at a small angle of attack-AoA) in the front and by lift generated by aft control surfaces (fins) and/or the vehicle body planing on the cavity. Viable vehicle control options are thus limited to actuation of the cavitator, fins and possibly thrust vectoring. Actuation of the cavitator offers the fastest control since the cavitator forces are larger than the forces on the other control surfaces. Fin control can also be considered fast, since multiple fins can be actuated simultaneously and fin lift increases with fin angle of attack, but has its limits in terms of attainable turn rates. Thrust vectoring, on the other hand, is only an option for slow control with large turn radii. Presently available fuel options (fuel energy density, fuel capacity) limit the vehicle to short flight times, therefore cavitator and/or fin control must be used. More details on the challenges of the control of supercavitating vehicles can be found for example in Kirschner et al. [1], Kuklinski et al. [2] and Stinebring et al. [3].

The interaction of the aft control surfaces with the cavity interface is nonlinear. Cavity shape and size, and vehicle position determine fin and/or vehicle immersion. This in turn determines the fin and planing forces acting on the supercavitating vehicle and thus vehicle dynamics, which interact with cavity dynamics.

This paper describes experiments that were carried out to study the complex interaction between the dynamics of a ventilated supercavity and the actuation of a fin control surface.

EXPERIMENTAL SETUP

Motion control hard- and software were combined with semi-axisymmetric, floor-mounted cavitators and a single wedge-shaped, 45 degree swept, cavity-piercing fin in the SAFL high-speed water tunnel to create the first version of a Control Surface-Cavity Interaction Simulator (CoSCIS, v.1). This setup, shown in Figure 1, was used for hydrodynamic fin-cavity interaction experiments and as a "hardware-in-the-loop" test bed for fin control strategies. The setup and experiments described here were developed and conducted at SAFL during 2005-06. Based on the experience and insight gained with this setup, a second-generation control test-bed (CoSCIS, v.2) was developed and used for experiments at SAFL during 2007-2009, as reported by Hjartarson et al. [4,5].
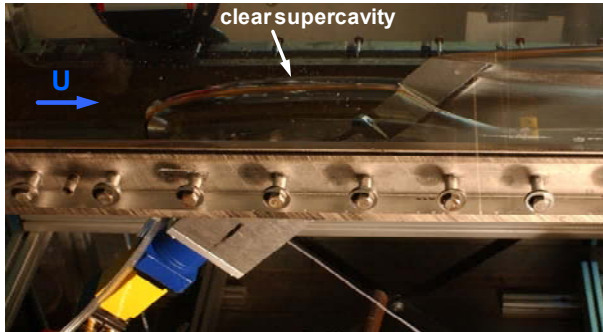
Figure 1a. CoSCIS, v.1 (Control Surface-Cavity Interaction Simulator) operating in SAFL high-speed water tunnel. Flow is left to right, main cavity and fin-base cavity are established.
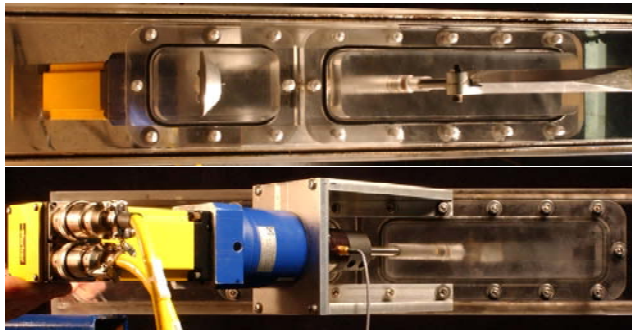
Figure 1b. CoSCIS, v.1 (Control Surface-Cavity Interaction Simulator) test bed. Top: top view, cavitator, swept fin. Bottom: view from below, motor, gearbox, torque cell.
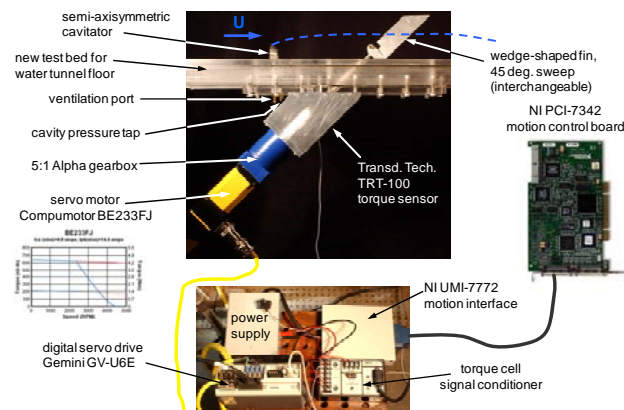
Figure 1c. CoSCIS, v.1 (Control Surface-Cavity Interaction Simulator): Water tunnel test bed and control hardware.

The CoSCIS v.1 test bed was connected to the water tunnel test section through two window inserts. On one insert various semi-axisymmetric cavitators could be mounted (with a small spacer elevating the cavitators to reduce wall effects on cavity shape), and a port for ventilation and a small tap for cavity pressure measurement were provided. Through the other insert, a 45-degree sweep interchangeable fin could be installed. The fin was mounted on a shaft at 25% of its chord, and actuated by a servomotor through a 5:1 gearbox, with a reactionary torque cell to measure fin torque. The fin was controlled by a programmable controller, which communicated with the servo motor through a National Instruments (NI) motion interface and a digital servo drive. NI LabVIEW and motion driver software were used to control the experiments and record data. Initially a NI PCI-7342 motion control board was used, which provided real-time P.I.D. control. However, in order to test fin control strategies it was soon replaced by a NI CompactRIO, which has an embedded customizable FPGA control and DAQ system and allows implementation of inversion control, receding horizon control (RHC), etc. The servo motor has a 2000 line optical encoder, the resolution of which is increased by a factor of four by the servo drive and by a factor of five by the gearbox, leading to a positioning accuracy of about 1/100 of a degree.

Figure 1a shows the hardware-in-the-loop test bed operating in the high speed water tunnel, with both a main supercavity and a fin base supercavity visible. Figure 1b shows the window inserts with cavitator and fin from the top, and a view from below of the motor, gearbox and torque cell. Figure 1c shows the test bed and the elements of the control hardware.

DISCUSSION OF RESULTS
Main cavity hysteresis

Initially four different semi-axisymmetric cavitator shapes were tested – a sharp-edged disk, a 30-degree cone, a 45-degree cone and a fore-shortened 45-degree cone – first without and then with a fin installed. It was found that a hysteresis exists for the establishment of the main supercavity at startup, similar to previous experiments with axisymmetric supercavities, cf. Wosnik et al. [6]. A hysteresis also exists for the establishment of fin base supercavities, but is typically less pronounced due to its smaller cavity volume. The transition regime between reentrant jet and twin vortex regimes has been well documented, e.g. Stinebring et al. [7], and experimental results for this hysteresis are not presented here. The data in the remainder of the paper are from experiments where the main cavity was generated with a sharp-edged disk cavitator.

The hysteresis in the establishment of the main supercavity at startup is shown in Figure 2. The non-dimensional ventilation gas flow rate, or air entrainment coefficient, has to be increased to 0.0634 before a clear supercavity is established (in this particular experiment this corresponds to a ventilation flow rate of 95 SLPM). Once the supercavity is established, the air entrainment coefficient can be decreased to 0.0365 (55 SLPM) before it disappears. Note that due to the semi-axisymmetric configuration, the cavitation numbers at which these transitions occur cannot be compared to the values commonly found for axisymmetric supercavities. Also note that due to the large cavity volume, the choking condition (cf. Tulin [8]) was reached at cavitation numbers σ_c^* of around 0.3.
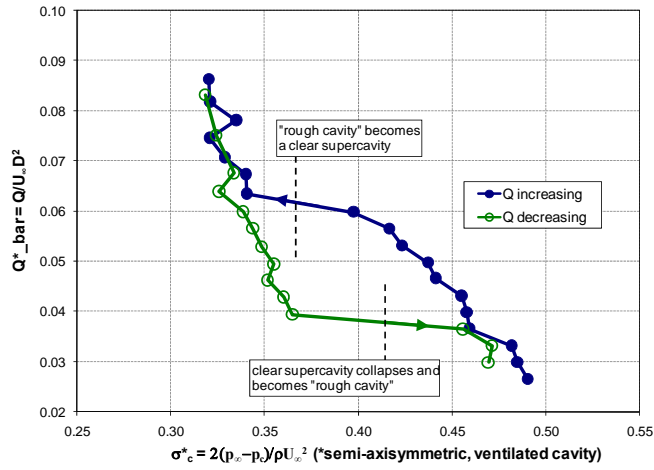
Figure 2: Example of observed hysteresis for the establishment of main supercavity.

The results of the hysteresis documented in this investigation and hysteresis documented previously [6,7] are summarized schematically in Figure 3 (for fin AoA=0°). A hysteresis exists for the establishment of the main supercavity (red). A hysteresis also exists for the transition between the re-entrant jet regime, where cavities are characterized by the shedding of toroidal vortices and the occurrence of non-stationary re-entrant jets, and the twin vortex regime, where cavities are dominated by gravity and ventilation gas is lost through two stationary vortex tubes (e.g., Cox and Clayden [9], Epshtein [10], Logvinovich [11]). A less pronounced hysteresis exists for the establishment of fin base cavities. The severity of the first two hystereses appears to be a function of total cavity volume. The hysteresis (green & red) becomes less significant with smaller total cavity volume, i.e., the larger the afterbody diameter is compared to the cavity diameter. However, when the torpedo cavity volume becomes small, the fin and fin base cavity hysteresis may become significant. Also, with reduced cavity volume there is less clearance between vehicle and cavity interface, which may be problematic during maneuvers. Note that once the fin is actuated (fin AoA≠0°) additional hysteresis exists when the fin becomes supercavitating from the leading edge, as will be shown in the next section.
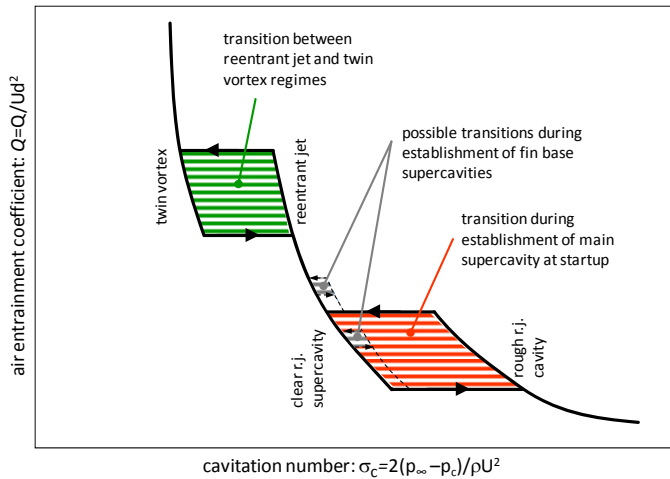

Figure 3: Schematic of observed hysteresis for cavity and fins, at zero fin angle of attack.

Fin forces and fin supercavity hysteresis

When a fin pierces the main supercavity, the protruding control surface can be either fully wetted on the suction side at small angles of attack, exhibit transitional partial cavities originating from the leading edge or have supercavities originating from the leading edge at higher angles of attack. These different types/stages of fin cavities are shown schematically in Figure 4. In all cases, a fin base supercavity will also exist. Figure 5 shows an example of the cavity-piercing fin during actuation: Vaporous, partial cavities form from fin leading edge and upper rear edge, while a large fin base artificial supercavity is maintained throughout. Fin control is highly nonlinear due to the interaction of the fin and fin-generated supercavities with the main supercavity wall.
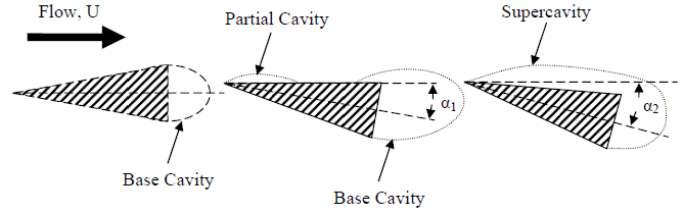
**Figure 4:** Different types of fin cavities during actuation.
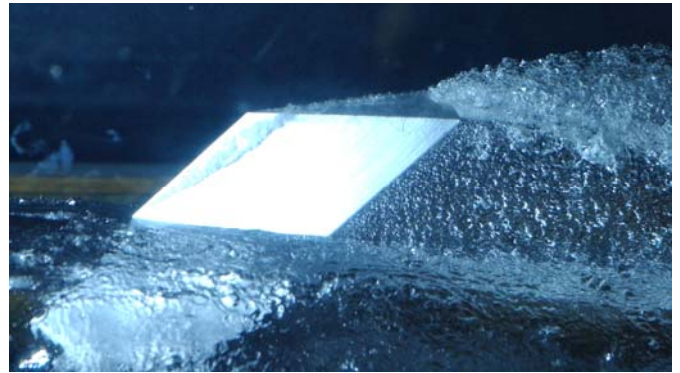
Figure 5: Cavity-piercing fin during actuation: Vaporous, partial cavities on fin leading edge and upper rear edge; large fin base ventilated (artificial) supercavity.

Fin torque was measured by varying the angle of attack in discrete 1° or 2° increments. The fin torque (lift) data for one test condition (U=9.4 m/s, Q=120 SLPM) are shown in Figure 6. For small angles of attack, with the suction side of the fin fully wetted, the data agree well with classical thin airfoil theory. Theoretical fin lift and torque can be calculated the following way: In classical thin, symmetrical airfoil theory the aerodynamic and pressure centers are at 0.25 chord c. For a wedge-shaped foil as the one used here the pressure center will be somewhat different from $0.25c$, and there will be a torque T, which at small AoA is mainly due to lift L, times moment arm a_1, taken with respect to the fin axis, which is at $a_0=0.25c$, $T=L\,a_1$. Lift L can be calculated with the lift coefficient for thin airfoil theory, $c_L=2\pi\alpha$. Then the moment arm a_1 was adjusted until the calculated torque in the fully wetted region matched the measured torque data. Plotted in Figure 6 (green line) is classical thin airfoil theory torque for $a_1=0.017c$. Once a supercavity exists from the leading edge of the fin, theoretical torque can be calculated from supercavitation theory in the same manner, $T=L\,a_2$, but with $c_L=\pi/2\,\alpha$ (for $\sigma=0$). Plotted in

Figure 6 (brown dashed lines) is supercavitation theory torque for $a_2=0.096c$. It can be concluded that for this test condition, as calculated from ideal theories, the pressure center moves from 26.7% chord (a_0+a_1) to 34.6% chord (a_0+a_2) when the wedge-shaped fin transitions from fully wetted to supercavitating from the leading edge. As expected, the pressure center of the fin moves further downstream for the supercavitating case.
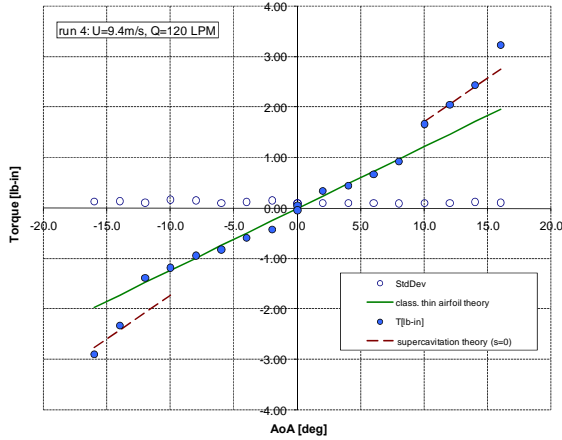

Figure 6: Fin torque (lift) measurement for discrete angles of attack (1 lb-in = 0.113 Nm).

Further, for this test condition a hysteresis of up to 4° angle of attack between the establishment and the disappearance of the fin supercavity was observed, cf. Figure 7. A supercavity from the fin's leading edge will establish itself at +/- 14° when AoA is increased, but will persist down to +/- 10° when AoA is decreased. Once a fin configuration for an actual vehicle has been specified, the hysteresis bounds need to be established for that configuration for various operating conditions, and the fin force data must be included in control algorithms.
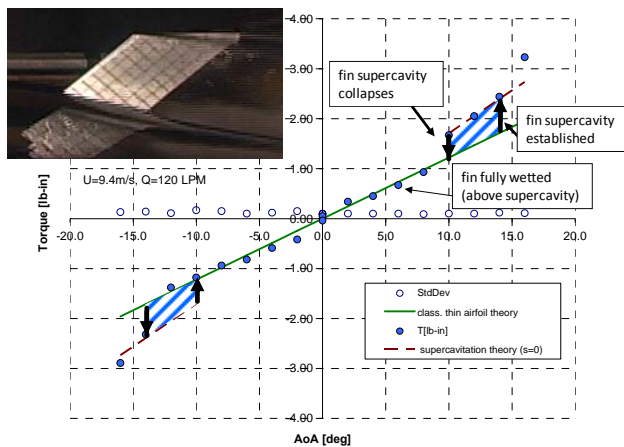
Figure 7: Fin torque (lift) measurement with supercavity establishment/collapse hysteresis. Inset: supercavitating fin (in hysteresis region).

For a different set of tests constant torque was applied to the fin in fixed increments. An example of these torque control tests is shown in Figure 8, where torque is increased and then decreased in 0.25 lbf-in steps for test conditions of U=9.6 m/s and Q=80 SLPM.
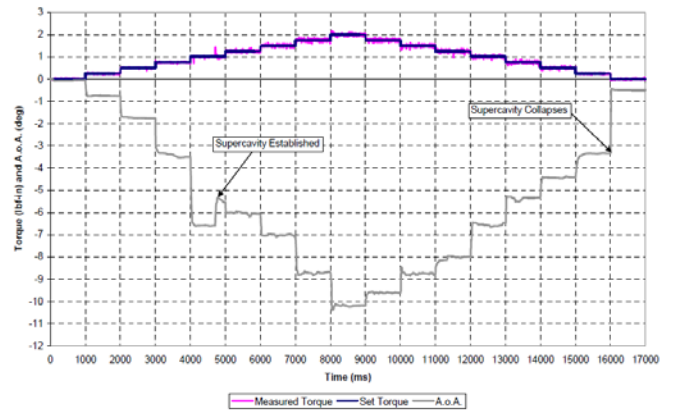
Figure 8: Torque control test. Constant fin torque is applied in 0.25 lbf-in increments (1 lb-in = 0.113 Nm).

In this case, the fin develops a supercavity from the leading edge while holding 1 lbf-in torque at approximately 6.5° AoA. With the supercavity established, the fin can hold the same torque at approximately 5.5° AoA. When decreasing torque, the supercavity persists down to 0.25 lbf-in torque and approximately 3.5° AoA, giving further evidence to the fin hysteresis shown in Figure 7. What was surprising was that at lower ventilation rates fin leading edge supercavities appear at lower angles of attack. Further, a significant time delay in the appearance and desinance of fin supercavities was observed. Both observations combined lead to the conclusion that the development and collapse of a fin leading edge supercavity is not just a function of fin angle of attack.

Figure 9 shows pictures of the various types of cavities observed on the actuated fin, as previously discussed and sketched in Figure 4.

Figure 9: Different types of fin cavities during actuation. Left: small AoA, base cavity only. Middle: intermediate AoA, partial cavity from leading edge. Right: larger AoA, supercavity (clear) from leading edge.

Stability of marginal cavities

If a "marginal" supercavity is disturbed it may find a "shortcut" through the hysteresis region and collapse. A marginal cavity is defined as a supercavity on the left, decreasing ventilation branch of the hysteresis regime, as shown in Figure 10. This situation occurs, for example, during maneuvers, when ventilation demand increases due to fin control surface actuation. A previously well-established supercavity can become marginal, and, when further disturbed by control surface actuation, collapse.
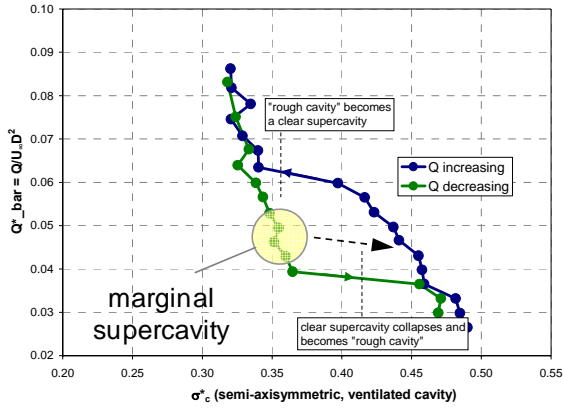
Figure 10: "Marginal" supercavity on left branch of hysteresis region of main supercavity.

Stability tests of marginal supercavities were conducted. The fin was initially moved to 15° AoA , simulating a maneuver, and then moved back to 0° AoA at a prescribed angular velocity. Prior to moving back to 0° AoA, however, the fin oscillated between +/- 15° AoA at 11 Hz for 10 cycles to simulate further cavity disturbances. For all cases the water velocity was U=9.6 m/s and the ventilation rate was Q=60 SLPM, near the minimum ventilation flow rate required to maintain the main body supercavity (cf. Figure 2).

Different angular velocities for moving to target AoA=0° were investigated. For example, fast angular motion (20 RPM, or 2.1 rad/s) to target AoA=0° caused the supercavity to become unstable and collapse, as shown in Figure 11 (data, high RMS fin torque after loss of supercavity) and 12 (photo of final outcome). Highly energetic re-entrant jets formed on the disturbed cavity surface, penetrated upstream and reached the front of the vehicle (cavitator), and destroyed the supercavity. In contrast, slow angular motion (2 RPM, or 0.21 rad/s) to target AoA=0° stabilized the main supercavity, as shown in Figure 13 (data) and 14 (photo of final outcome). The results discussed here were highly repeatable for different operating conditions. It appears that slow angular motion to target AoA is a key to preventing highly energetic re-entrant jets from forming and maintaining supercavities in the marginal stability region. Note in Figures 11 and 13 that the controller overshot to oscillation angles somewhat higher than ±15°.

In summary: If a marginal supercavity is disturbed by fin actuation, fast motion to fin target AoA can lead to the loss of the supercavity (and hence loss of the vehicle), whereas slower motion to target AoA tends to stabilize the supercavity.
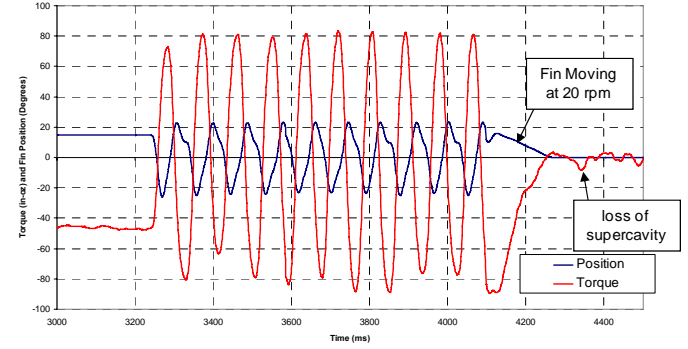
Figure 11: Control surface actuation with fast motion (20 RPM) to target AoA=0° after an 11 Hz disturbance - marginal supercavity collapses (=loss of vehicle). (20 RPM=2.1 rad/s)
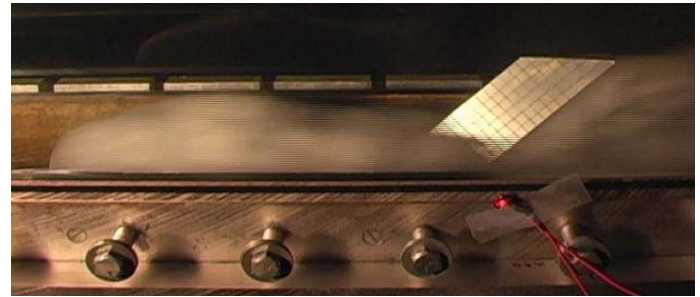
**Figure 12:** Collapse of marginal supercavity after fast control surface motion to target AoA.
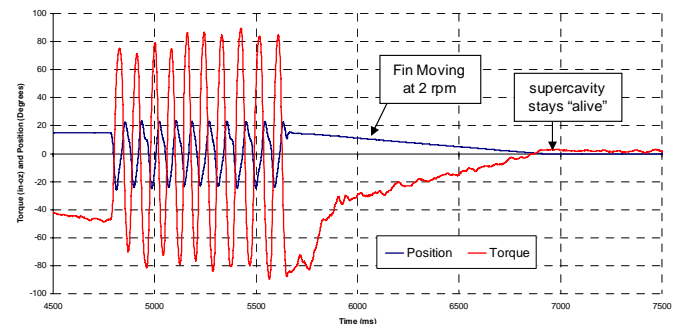
Figure 13: Control surface actuation with slower motion (2 RPM) to target AoA=0° after an 11 Hz disturbance - marginal supercavity survives. (2 RPM = 0.21 rad/s)

Figure 14: Stabilization and survival of marginal supercavity after slow control surface motion to target AoA.
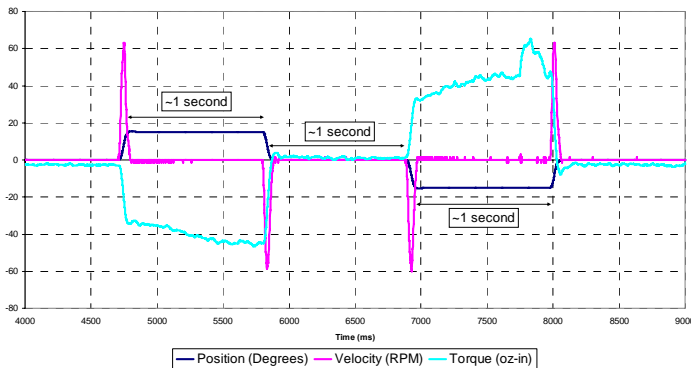
Simple control maneuvers

An example of a simple fin control experiment simulating an obstacle avoidance (lateral shift, S-shape) maneuver is shown schematically in Figure 15, and the data are presented in Figure 16. CoSCIS v1 allows a water tunnel simulation of the actuation of the fin perpendicular to the drawing plane. For this experiment, the water velocity was U=9.6 m/s and the ventilation rate was Q=60 SLPM.

fins being actuated
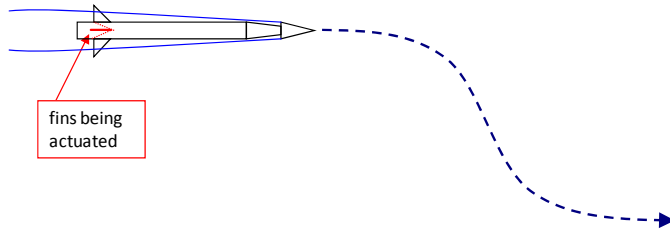
Figure 15: Schematic of a simple supercavity-piercing fin control maneuver (obstacle avoidance/lateral shift).

The controller steps the fin through an angular motion sequence moving to four target AoAs: positive target (15°) for one second, 0° for one second, negative target (-15°) for one second and back to 0°.

Figure 16: CoSCIS v1 data from a simple supercavity-piercing fin control maneuver (obstacle avoidance/lateral shift).

SUMMARY

Experiments were conducted with a semi-axisymmetric, ventilated supercavity and a single wedge-shaped, 45 degree swept, cavity-piercing fin. Several phenomena were identified that warrant further study and incorporation into control models. These include the hysteresis of fin supercavities with respect to fin angle of attack, the increased ventilation demand as fin control surfaces are actuated, and concerns about main supercavity stability upon fin actuation. The results, and the experience and insight gained from these experiments led to the design of a more advanced control experiment, CoSCIS v.2.

ACKNOWLEDGMENTS

REFERENCES

[1] Kirschner IN; Uhlman JS; Perkins JB (2006) Overview of High-Speed Supercavitating Vehicle Control. AIAA Guidance, Navigation, and Control Conference and Exhibit, Keystone, CO (AIAA-2006-6442)

[2] Kuklinski R; Fredette A; Henoch C; Castano J (2006) Experimental Studies in the Control of Cavitating Bodies. AIAA Guidance, Navigation and Control Conference and Exhibit, Keystone, CO (AIAA-2006-6443)

[3] Stinebring DR; Cook RB; Dzielski JE; Kunz RF (2006) High-Speed Supercavitating Vehicles. AIAA Guidance, Navigation and Control Conference and Exhibit, Keystone, CO (AIAA-2006-6441)

[4] Hjartarson A; Hambleton W; Balas G; Arndt REA (2007) A dynamic test platform for evaluating control algorithms for a supercavitating vehicle. 60th Annual Meeting of the Division of Fluid Dynamics, Salt Lake City, Utah

[5] Hjartarson A; Mokhtarzadeh H; Kawakami E; Balas G; Arndt REA (2009) A dynamic test platform for evaluating control algorithms for a supercavitating vehicle. Proceedings of the 7th International Symposium on Cavitation, CAV2009, Ann Arbor, Michigan, USA.

[6] Wosnik M; Schauer TJ; Arndt REA (2003) Experimental Study of a Ventilated Supercavitating Vehicle. Paper Cav03-OS-7-008, CAV 2003-Fifth International Symposium on Cavitation, Osaka, Japan.

[7] Stinebring DR; Billet ML; Holl JW (1985) "An Experimental Study of Cavity Cycling for Ventilated and Vaporous Cavities," International Symposium on Jets and Cavities, ASME, Miami Beach, FL

[8] Tulin MP (1961) *Supercavitating Flows.* In Streeter, V. (ed.), Handbook of Fluid Dynamics, McGraw-Hill, New York, pp. 12-24 to 12-46.

[9] Cox RN; Clayden WA (1956) Air entrainment at the Rear of Steady Cavity. Proceedings NPL Symposium on cavitation in Hydrodynamics – 1955, paper v12, HMSO, London 1956.

[10] Epshtein LA (1973) Characteristics of ventilated cavities and some scale effects. Proceedings of IUTAM Symposium in Leningrad: "Unsteady Flows of water with high speeds" - 1971, NAUKA-1973, pp.173-185. (translated to English from Russian)

[11] Logvinovich GV (1969) Hydrodynamics of Flows with Free Boundaries, NAUKOVA DUMKA, Kiev, 215p. (translated to English from Russian)